

Author's Accepted Manuscript

Extending the applications of sediment profile imaging to geochemical interpretations using colour

P.J. Statham, W.B. Homoky, E.R. Parker, J.K. Klar, B. Silburn, S.W. Poulton, S. Kröger, R.B. Pearce, E.L. Harris



www.elsevier.com/locate/csr

PII: S0278-4343(17)30447-8
DOI: <https://doi.org/10.1016/j.csr.2017.12.001>
Reference: CSR3701

To appear in: *Continental Shelf Research*

Received date: 24 August 2017
Revised date: 24 November 2017
Accepted date: 3 December 2017

Cite this article as: P.J. Statham, W.B. Homoky, E.R. Parker, J.K. Klar, B. Silburn, S.W. Poulton, S. Kröger, R.B. Pearce and E.L. Harris, Extending the applications of sediment profile imaging to geochemical interpretations using colour, *Continental Shelf Research*, <https://doi.org/10.1016/j.csr.2017.12.001>

This is a PDF file of an unedited manuscript that has been accepted for publication. As a service to our customers we are providing this early version of the manuscript. The manuscript will undergo copyediting, typesetting, and review of the resulting galley proof before it is published in its final citable form. Please note that during the production process errors may be discovered which could affect the content, and all legal disclaimers that apply to the journal pertain.

Extending the applications of sediment profile imaging to geochemical interpretations using colour

P.J. Statham^a, W.B. Homoky^b, E.R. Parker^c, J.K. Klar^{a,d}, B. Silburn^c, S.W. Poulton^e, S. Kröger^c, R.B. Pearce^a, E.L. Harris^a

^aOcean and Earth Science, University of Southampton, National Oceanography Centre, Southampton, SO14 3ZH, United Kingdom

^bUniversity of Oxford, Department of Earth Sciences, South Parks Road, Oxford, OX1 3AN, United Kingdom

^cCentre for Environment, Fisheries and Aquaculture Science, Pakefield Road, Lowestoft, NR33 0HT, United Kingdom

^dPresent address: LEGOS, Université de Toulouse, CNES, CNRS, IRD, UPS, 14 Avenue Edouard Belin, 31400 Toulouse, France

^eSchool of Earth and Environment, The University of Leeds, Leeds. LS2 9JT, United Kingdom

Corresponding author: email pjs@soton.ac.uk

Keywords: iron, manganese, shelf sediments, SPI colour, geochemistry

Abstract

Whilst Sediment Profile Imaging (SPI) is a very widely used technique in the regulatory assessment of seabed environmental health, and in the study of seafloor sediment-biology interactions, the potential for SPI images to be used in a geochemical context has not been rigorously assessed. Here we have examined relationships between colour and geochemistry in a sediment core collected from the Celtic Sea, North West European Shelf, that was digitally imaged and on which detailed geochemical analyses were also performed. Average oxygen penetration depth was 4.08 ± 0.72 mm, (n=5), whilst the apparent redox potential discontinuity (aRPD) as determined by sediment colour change was at 78 mm. As iron (oxyhydr)oxides decreased with depth, black sulfide phases increased, and the aRPD most closely correlated with this geochemical change rather than the oxygen penetration depth. Colour analysis of the image showed a clear correlation of brightness with black FeS (acid

volatile sulfide). There was a general correlation of iron oxide phases with orange colour in the upper part of the sediment profile, whilst in the lower part of the core the orange oxide phases appeared to be obscured by the black FeS present. The sulfide-brightness relationship indicates colour analysis can provide an estimate of FeS, and potentially the carrying capacity for toxic metals such as cadmium, zinc and copper as sulfides in this type of sediment. Additionally, detailed geochemical analyses of SPI cores may provide new insights into the activity and impacts of infauna and the link with sediment biogeochemical cycles of carbon and nutrients.

1. Introduction

The development of the *in situ* sediment profile imaging (SPI) technique has provided a powerful tool for rapid spatial assessment of biological activity in surface sediments (Rhoads and Cande, 1971). The SPI approach is now widely used for assessing environmental quality parameters (Germano et al., 2011; Solan et al., 2003) in general and also in relation to national and international standards. These applications are based on data from the images being used with current conceptual models of sediment-organism relationships

An important parameter first derived from the SPI images in the 1970s was a redox potential discontinuity (RPD) corresponding to colour changes and assumed variations in geochemistry (Fenchel, 1969; Vismann, 1991). However, the RPD subsequently became synonymous with biological mixing depth on the premise that the colour transition was biologically mediated. The RPD was then used in gauging the ecological health within successional models, and was subsequently used in the derived indices of Benthic Habitat Quality (Rosenberg et al., 2004) and the Organism-Sediment Index (Rhoads and Germano,

1986). Whilst microbial communities associated with burrow structures do appear to be linked to availability of oxidants (Bertics and Ziebis, 2009), little other data supports a strong link between macro organism mixing depth and the RPD. The realisation of this limitation led to the use of “apparent RPD” to describe the colour transitions seen. As measurements of the redox potential, or *in situ* oxygen and other redox variables such as iron or nitrate, are not possible with current SPI technology, it has been assumed that reddish-brown sediment colour tones are indicative of sediments in an oxidative geochemical state, and that the sediment porewaters are not intensely reducing. The rigorous interpretation of the aRPD in relation to oxidising conditions thus remains difficult (Gerwing et al., 2015), and despite the effort expended in obtaining these images only limited work has been done on exploring the potential to use such images for geochemical investigations (Grizzle and Penniman, 1991; Teal et al., 2009), and then largely on solute phases of sediment chemistry rather than the particulate components which may contribute the bulk of the colour observed .

A direct approach to providing improved metal biogeochemical data used chemical sensors incorporated into the SPI system (Teal et al., 2013; Teal et al., 2009). The diffusive gradients in thin films (DGT) technique applied provides fluxes of dissolved Fe and Mn from sediment to the collection gel. Whilst useful data on time integrated liberation of dissolved Fe and Mn in the sediment matrix is provided, as the measurements are done *in situ* it is not possible to relate fluxes to the oxygen penetration depth, or porewater and solid phase composition.

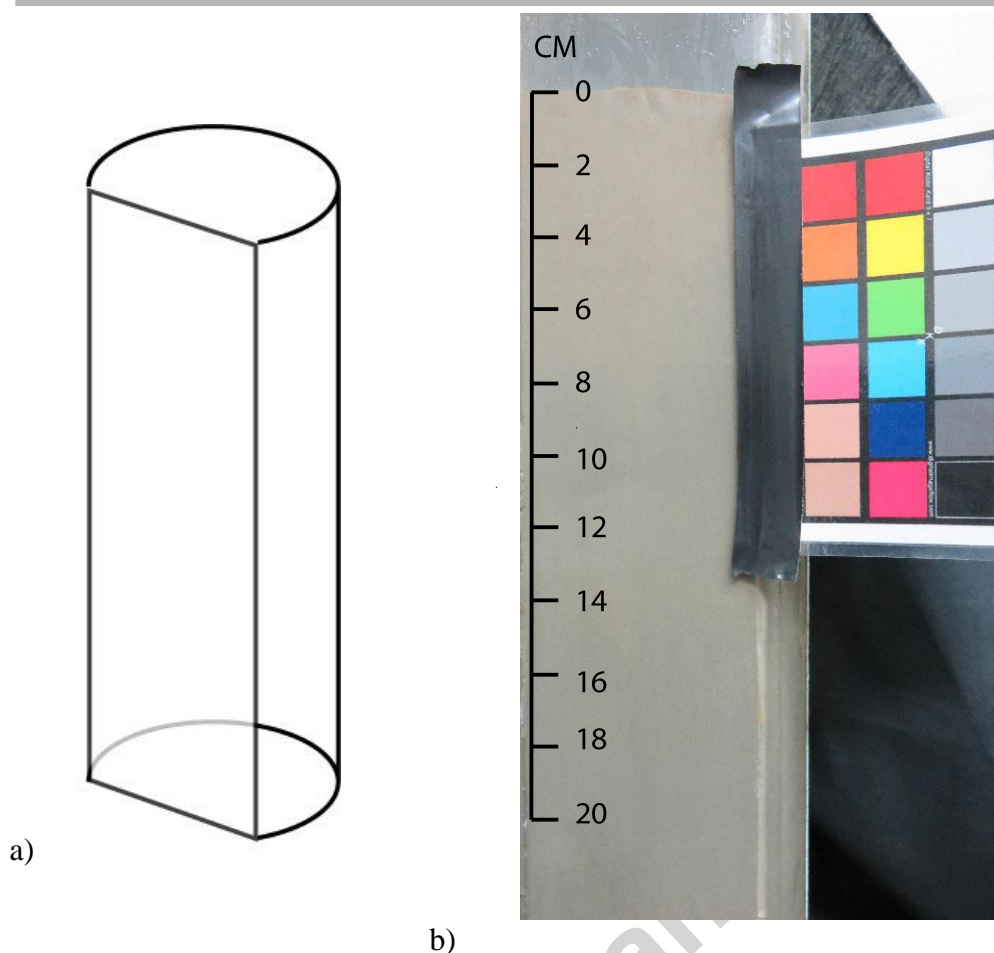
Here we have taken the novel approach of collecting a core that was digitally imaged and also geochemically analysed by a wide range of techniques to provide data on porewater and solid phase parameters. This approach allows a direct comparison of image and sediment geochemistry at this shelf site, and provides a rigorous basis for assessing the potential of

using SPI images in a geochemical context. Additionally the geochemical signatures can provide insights into linked biogeochemical cycles and biological processes occurring (Bertics and Ziebis, 2009).

2. Methods

The work was carried out within the framework of the NERC funded Shelf Sea Biogeochemistry Programme. A NIOZ box corer was used at cohesive Site A (sandy mud, ~51° 12.6754' N, 6° 8.0277' W) within the Celtic Sea, UK (Thompson et al., 2017) in August 2015. The NIOZ collected sediment was sub-sampled using a modified 10 cm diameter core tube (Figure 1a) in which a flat sheet of transparent polymethyl methacrylate replaced part of the tube wall. The flat face allowed a digital image to be taken under laboratory lighting using a Canon G15 camera (12.1 megapixel CMOS detector) of a cross section of the core (Figure 1b; see supplementary material for a high-resolution [637 × 2577 pixels, 300dpi] image file). A standard colour card (Digital Kolor Kard from digitalimageflow.com) was photographed at the same time for scale and colour inter-comparison.

Figure 1. a) Modified core tube. Original tube size 10 cm diameter by 60 cm long) b). Colour image of core, showing depth scale and reference colour card used.



The aRPD was determined following a published procedure (Solan et al., 2004). Here the image is analysed using the open access Image-J programme, in which the image is broken down into RGB colours, the red channel chosen and the range of intensities selected to best highlight the colour change associated with the aRPD.

A detailed description of most sampling and analytical techniques used is provided elsewhere (Klar et al., 2017) and only an overview is given here, except for those techniques not covered in the Klar et al. paper. The strategy was to choose analytes that indicate the redox state of the core, and solid phases that would impact colour (thus for example iron (oxyhydr)oxides would be expected to be an orange colour and initially formed under oxidising conditions, whilst FeS is black and is indicative of typically reducing conditions).

Replicate dissolved oxygen profiles across the core surface were collected behind the flat wall of the core tube before any subsampling was done. A Unisense Clark type electrode with a 100µm tip was used, and data on oxygen was obtained at typically 200µm depth intervals across the benthic interface and into the sediment. With core top water removed, porewaters were extracted from the sediment core at typically 1 to 2 cm depth intervals using Rhizon samplers (Seeborg-Elverfeldt et al., 2005) that prevent oxygen contamination of the collected porewaters (*c.f.* Klar et al. 2017). After porewater extraction and filtration, the residual sediment was sliced using a polycarbonate sheet at 0.5, 1 and 2 cm depth-intervals, and stored at -20° C in zip-lock bags prior to further analyses.

The concentrations of Fe(II), and Fe(II) plus Fe(III) (i.e. after addition of a reducing agent), were determined in the dissolved (<0.15 µm) size fractions of porewater samples using the Fe(II)-complexing ferrozine ligand (Sigma-Aldrich) (Stookey, 1970; Viollier et al., 2000). In order to examine associations of Fe and Mn with solid sediment phases, firstly an ascorbic acid leach (Raiswell et al., 2010) was used to extract the easily reducible oxide phases, such as amorphous ferrihydrite, but not the more crystalline oxide phases. A further citrate dithionite reducing leach was then applied to each sample to remove more crystalline Fe oxide phases including haematite and goethite (Poulton and Canfield, 2005; Raiswell et al., 1994). The total dissolution of non-leached freeze dried and ground sediment samples used a mixture of hydrofluoric, nitric and hydrochloric acids in PFA containers on a hotplate. Fe and Mn in the leach solutions were determined using an inductively coupled plasma optical emission spectrometer (ICP-OES, iCAP6000 Series, Thermo Scientific). Nutrient concentrations in sediment porewaters were all analysed on board using a Bran and Luebbe segmented flow colorimetric auto-analyser (Woodward and Rees, 2001). Particulate organic carbon (POC) and nitrogen (PON) were determined using a Carlo-Erba CHNOS analyser (Nieuwenhuize et al., 1994).

In order to determine the major mineral phases present X-ray diffraction analysis of the sediment was done using a PANalytical X'Pert pro diffractometer machine fitted with a Cu X-ray tube. The machine operating conditions were 35kV, 40mA utilising automatic slits and a step size of $0.02^\circ 2\theta$ at 1 second/ step. The samples were prepared as randomly oriented powder samples with an internal standard of 25% by weight of corundum and side-loaded to avoid preferred orientation. Precision values for the samples are approximately ± 0.5 -2% for crystalline materials and ± 10 -20% (of the amount present) for total clay. Scanning electron microscope work used a Carl Zeiss LEO1450VP Scanning Electron Microscope (SEM) fitted with an Oxford Instruments EDS system, and an X-Act Silicon Drift Detector (10mm^2 area) using the AZtec Energy software system (v.3.1).

Acid volatile sulfide (AVS) and pyrite (PY) were determined in the sediment following the approach of Canfield et al. (1986) using a sequential acid (6M HCl) reflux, and then acidified chromous chloride reflux, to convert the solid phase sulfides to hydrogen sulfide that is collected as silver sulfide (Ag_2S) in a silver nitrate solution. The two sulfide pools in the sediment are calculated after gravimetric measurement of the Ag_2S formed from the known mass of sediment added.

Analysis of the core colour was based on the iron (oxyhydr)oxides appearing in the red-orange part of the spectrum (haematite and ferrihydrite are red-orange, goethite is orange) and iron mono-sulfides (FeS ; AVS) being black and impacting image brightness. Colour analysis was done using the open access ImageJ suite (Fiji implementation). In order to compare brightness with measured AVS concentrations, the image was first converted to a hue-saturation-brightness (HSB) stack, and the brightness layer examined. Brightness values

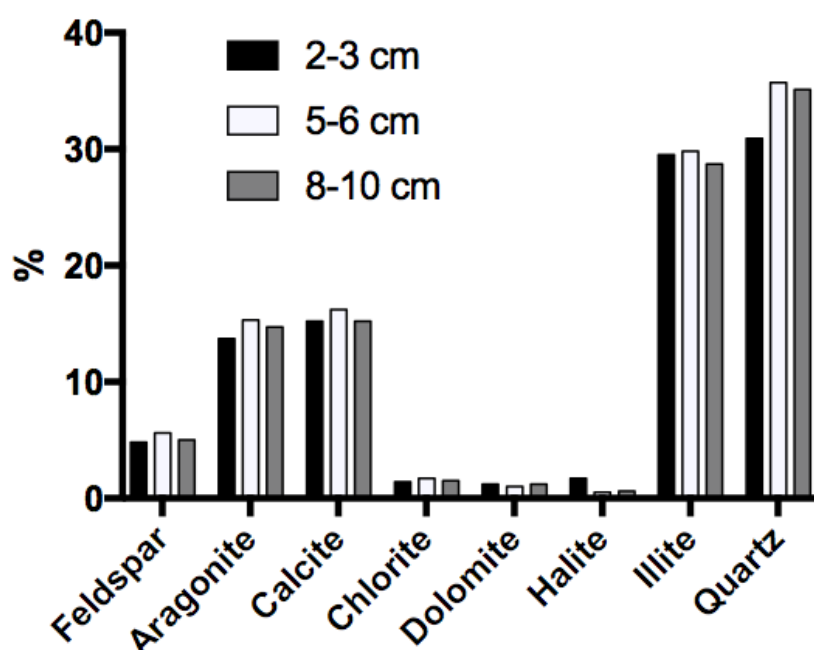
were read off at 5 points across the image at the sampled depth, and averaged to provide a value to plot against AVS. For the iron (oxyhydr)oxide phases, the zone in the image corresponding to the geochemical analysis was selected and the colour threshold selected to correspond to orange values. Digital values of 20-37 bracketing the orange range (circa 590-620 nm) were chosen and pixels in this range were picked out on the image. The image was then analysed for the fraction of pixels that corresponded to the orange range. The fractions were then compared to the corresponding iron (oxyhydr)oxide data.

3. Results and Discussion

3.1 Bulk composition

Site A is a very poorly sorted, very fine skewed, mesokurtic, very coarse silt, classified according to the Folk classification scheme as a sandy mud; see Thompson et al. (2017) for further detail. Major components of the sediment matrix are shown in Figure 2.

Figure 2. Bulk mineralogy of the core at discrete depths.



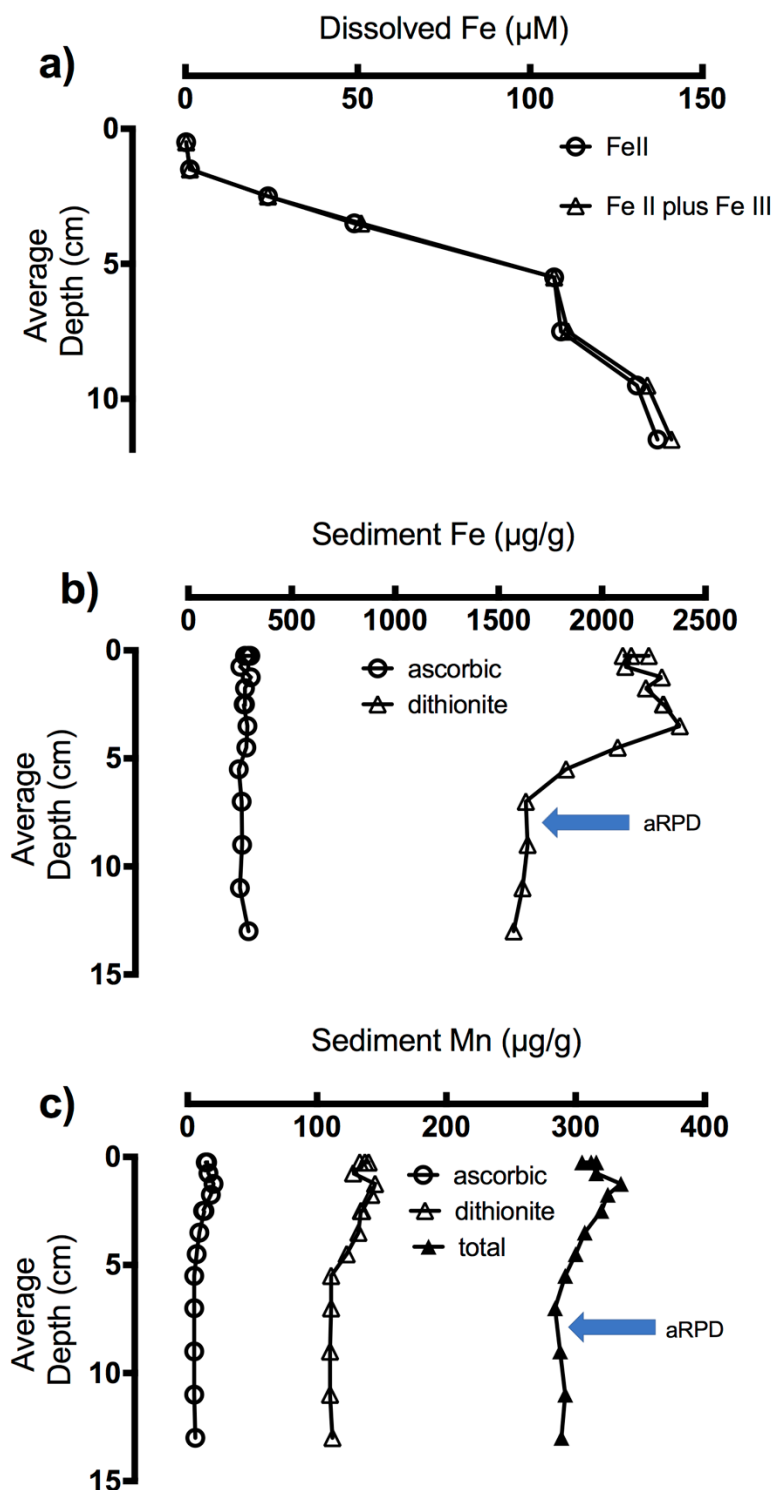
Dominant mineral phases are carbonates (primarily aragonite and calcite), quartz, illite, and feldspar; changes in these components with depth are small. The carbonate fractions are expected to come from two sources. Firstly, eroded Cretaceous carbonaceous rocks would have been transported here during the last Ice Age when the major river system running through what is now the English Channel deposited a fraction of its particle load. Secondly, carbonate will have been generated by the ubiquitous shelled organisms amongst the benthos living within the surface sediments. The independent particulate inorganic carbon data is in reasonable agreement with the XRD data (averages of 36.5 and 30.6% respectively). Particulate organic carbon (average 1.05%; see supplementary material) is a small component of the total carbon in this matrix, and remains fairly constant with depth except for a small increase towards the surface. The quartz, feldspar and illite are products of lithogenic erosion and weathering.

3.2 Redox status of the core

In accordance with the accepted general diagenetic sequence of terminal electron acceptors (Burdige, 2006) oxygen and then nitrate rapidly disappear in the upper few mm of the core. Measured oxygen penetration depths (4.08 ± 0.72 mm, $n=5$) are more than an order of magnitude shallower than the aRPD (78 mm). Further degradation of organic carbon is expected to sequentially use Mn and Fe oxides and then sulfate as electron acceptors. Mn oxides can be important electron sinks when present at high enough concentrations (Thamdrup et al., 1994). However, in this core average total Mn (297 $\mu\text{g/g}$) is only 2.1 % of average total Fe (14110 $\mu\text{g/g}$) on a mass/mass basis, and the reducible Mn oxides (dithionite released) are at low concentrations relative to the equivalent Fe oxide phases (127 c.f. 2027 $\mu\text{g/g}$). Thus iron (oxyhydr)oxides are expected to be the most important electron acceptors.

Porewater dissolved Fe(II) (dFe(II)) follows the trends expected with very low concentrations near surface, where iron oxidation is possible, increasing down to about 6 cm, followed by high and relatively constant dFe(II) concentrations deeper in the core (Figure 3a).

Figure 3 a) Dissolved ($<0.15\ \mu\text{m}$) Fe, b) ascorbic acid and dithionite leachable Fe, c) Mn total, ascorbic and dithionite leaches.



Isotope data demonstrates that this dFe(II) is predominantly derived from bacterial dissimilatory iron reduction (DIR) (Klar et al., 2017). A further route for formation of FeII in solution is the reaction between HS^- and iron oxides (see below). Porewater nutrients follow

anticipated patterns with nitrate rapidly disappearing in surface sediments, followed by an increase in ammonium, phosphate and dissolved silicon with depth (see supplementary material).

3.3 Solid metal phases within the sediment core

Total Fe and Mn in sediments (averages 1.41 % and 306 $\mu\text{g/g}$ respectively) are low relative to continental crustal values of 5.13% for Fe and 852 $\mu\text{g/g}$ for Mn (Albarede, 2003). This reflects dilution with illite (variable Fe content but nominally 1.43%), carbonate (normally regarded as a relatively pure diluent in analysis of geological matrices), and quartz. Quartz typically has low concentrations of trace metals and most Fe associated with the mineral is as oxide coatings. Any coatings would be released through the dithionite-citrate leaching techniques applied here (see below).

Leachable Fe falls into two groups:

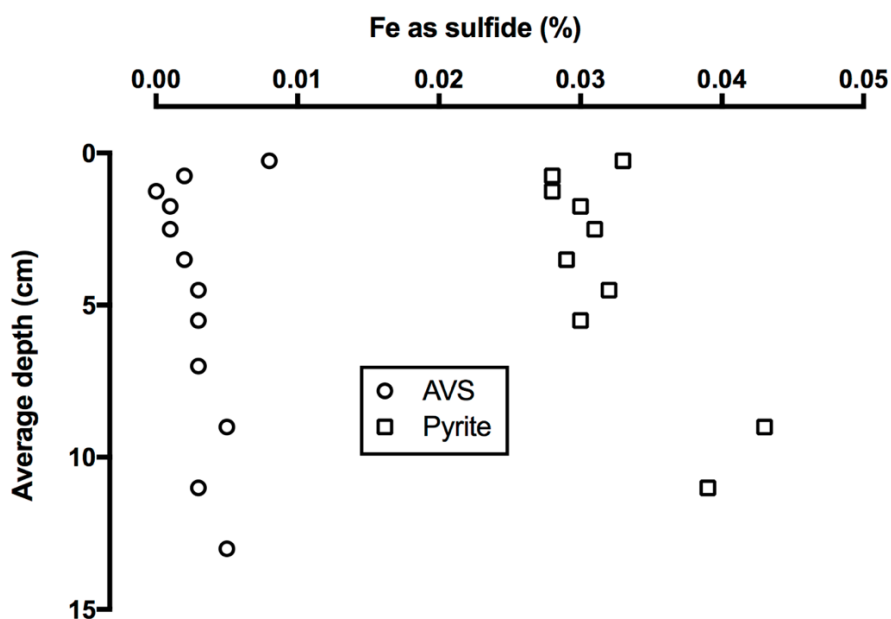
- 1) The ascorbic fraction that is reported to correspond primarily with amorphous ferrihydrite phases (Raiswell et al., 2010), remains relatively constant throughout the sampled core (average 274 $\mu\text{g/g}$, Figure 3b). This constancy is at first sight surprising as one would expect this geochemically reactive oxide phases to be rapidly reduced in the oxygen deficient zone beneath the surface few mm. In another core from this site (Klar et al., 2017) an increase in ascorbic Fe was noted just below the surface in the oxidised layer, reflecting precipitation of dissolved Fe diffusing upward, whilst average deeper concentrations were similar to those found here, demonstrating consistency at depth between cores. This low but consistent concentration of ascorbic leachable Fe throughout the core most probably reflects a

combination of primary ferrihydrite and iron that has been reduced at the surface of Fe oxides, but not yet released to solution (Poulton, 2003).

2) The dithionite-citrate reagent applied after the ascorbic leach will remove the more crystalline oxide phases including goethite and haematite (Poulton and Canfield, 2005; Raiswell et al., 2010). These phases are present at concentrations about an order of magnitude higher than that of the ferrihydrite (Figure 3b). The amorphous phases are expected to be the most geochemically reactive, and unless reduced they are expected to gradually reorder their structures to more crystalline forms. The other important Fe bearing non-lithogenic mineral phases in sediments are sulfides.

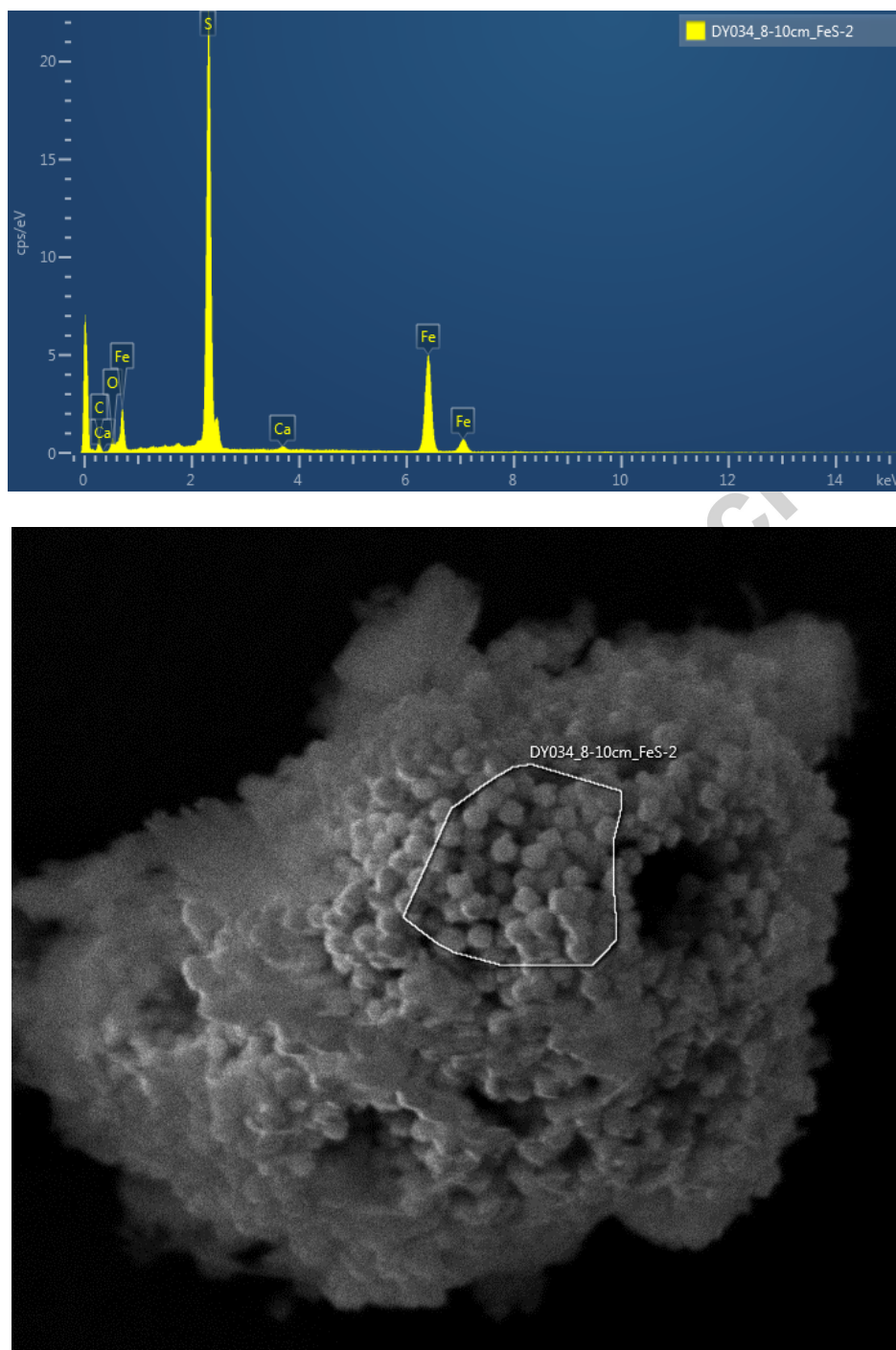
Bacterial sulphate reduction is reported for a range of similar temperate shelf and coastal environments when oxygen and other more energetically favourable terminal electron receptors are not available (Teal et al., 2009; Thamdrup et al., 1994), but the expected resulting dissolved sulfide was not detected at any of the sampled depths of a core taken at the same site (Klar et al., 2017). In this system any dissolved sulphide will rapidly react with both reduced FeII and reactive iron oxides to generate FeS that gives the black colour in reducing sediments (Bull and Williamson, 2001), and so dissolved sulfide will be consumed immediately after formation. Additional fates for HS^- include release of oxidised S species (Burdige, 2006), and mineralisation with any chalcophilic trace metals (e.g. Cd, Cu, Hg, Pb, Zn). The FeS transforms further to the more stable pyrite (FeS_2), which is the major long term sink for S in sediments (Burdige, 2006). In this core AVS (principally FeS) and pyrite are present at low concentrations (Figure 4).

Figure 4. Iron sulfide phases in the core.



Both sulfide phases gradually increase with depth, with the biggest increase occurring below the aRPD, and throughout the pyrite concentrations are an order of magnitude higher than the corresponding AVS values (Figure 4). Other intermediary Fe-S compounds exist that are only partially dissolved during our AVS treatment (greigite, Fe_3S_4), but these generally occur at much lower concentrations than FeS and pyrite. Pyrite is typically found in framboidal or euhedral forms as shown in the SEM image in Figure 5.

Figure 5. SEM-image of sediment at 8-10 cm in the core showing pyrite framboidal crystals (bottom) and EDS analysis of polygonal zone (top) shown in the SEM, confirming composition as FeS_2 (maximum width of polygon is $5\mu\text{m}$).



The amorphous Fe(oxyhydr)oxides formed by upwards diffusion of FeII and precipitation on reaching oxygen containing porewaters, will be a highly reactive phase with which the HS^- can react rapidly (Canfield et al., 1992; Poulton et al., 2004). Additionally organic rich

microniches can be sites of intensive redox reactions (Lehto et al., 2017). Therefore, the surface few mm of sediment can be an important formation site for FeS and FeS₂, consistent with the higher AVS and PY concentrations at the surface of this core (Figure 4). In addition to in situ formation, bioturbation may also transfer pyrite from deeper in the sediment to surface layers. The crystalline Fe oxides found deeper in the sediments will react more slowly with HS⁻ (Poulton et al., 2004) and HS⁻ production is typically slower here than in surface layers (Teal et al., 2009), which may lead to accumulation of HS⁻, but at depths greater than those studied here. The relatively low concentrations of solid sulfide phases and the presence of iron (oxyhydr)oxides at depth in the core indicate this sediment is reactive iron, rather than sulfur, dominated. In sediments where organic carbon supply is greater, and sulphate reduction is enhanced, greater concentrations of sulfides would be expected (Devereux et al., 2015).

Leachable Mn phases increase gradually above the aRPD (Figure 3c). The reagents with strongest reducing action (dithionite) released most Mn, and constituted on average 41.3% of the total values. These Mn reducible forms are therefore an important fraction of the total Mn present. The increase in these fractions above the aRPD is consistent with trapping of dissolved Mn as the more oxic surface conditions are approached, and downward biological mixing of surface formed Mn oxides (Thamdrup et al., 1994).

3.4 Linking solid phases and processes within the core to colour

The pure forms of the major constituents in the core (carbonate, illite, quartz) have no significant colour in the visible spectrum, and therefore act as a white “canvas” against which the colour from minor mineral components can be more readily seen. Sands that are

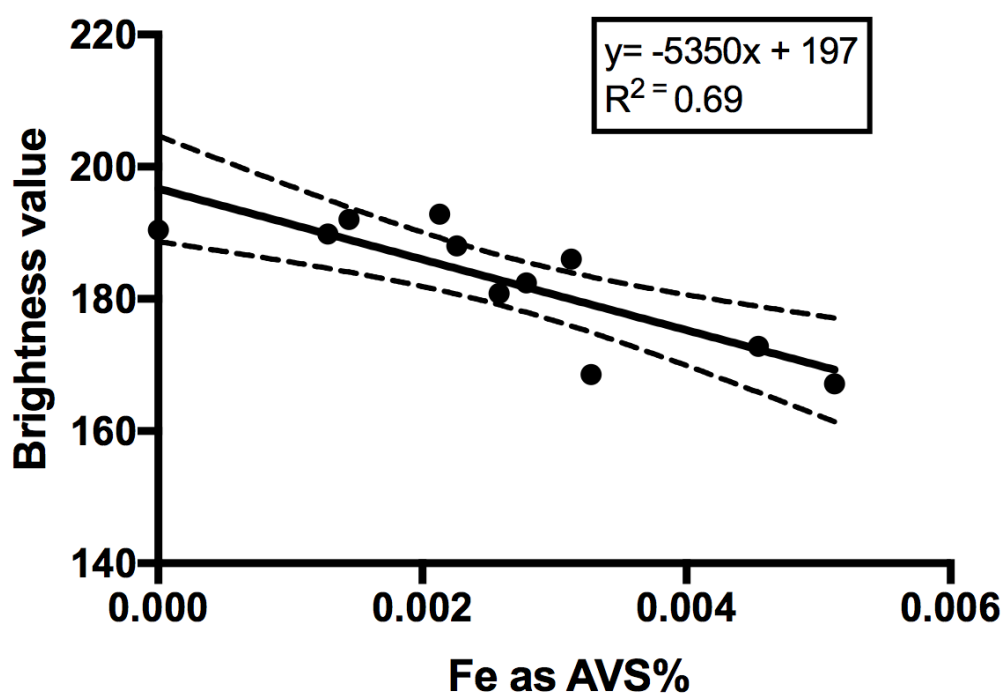
predominantly quartz may have a reddish hue due to surface Fe oxides that will be removed by the analytical procedures used here, and will thus be observed in the oxide fraction.

The main coloured minerals expected in this sediment matrix are iron (oxyhydr)oxides, and iron sulfides. The primary black coloured sulfide phase is expected to be an amorphous mono-sulfide that gives the colour to hydrothermal “black smokers”, and this mineral will be measured by the AVS technique. Although pyrite is more abundant than the AVS liberated sulfides, its colour is typically a muted gold, and can be found in framboidal crystalline forms (Figure 5). The main concentration changes for these minerals are around the aRPD depth at 7.8 cm (Figure 4). Above this depth, the dithionite Fe phases (expected to be mainly goethite and haematite) increase by ~27% to the surface whilst below, pyrite and AVS increase by ~25%.

In order to link these geochemical observations with core colour requires an appropriate methodological approach. The most useful starting point was the work of Bull and Williamson (2001) who investigated correlations between “amorphous” iron oxides and acid volatile sulfur and colour properties on core samples collected from an estuarine system; image analysis was used to generate colour intensity and colour saturation to compare, respectively, to AVS and iron (oxyhydr)oxide concentrations. The underlying rationale was to provide an image-based estimate of the binding capacity of the sediment for toxic metals such as Cu and Zn. Indeed, the need for such innovations that may improve the quantification of metal source-sink relationships in marine sediments has been identified (Homoky et al., 2016). A related image analysis approach was taken here.

When brightness is plotted against AVS (Figure 6), a reasonable negative correlation is seen, despite the shelf core having a smaller range of intensity values than the estuarine core of Bull and Williamson (2001). The surface-most sample that has relatively high values for both AVS and pyrite appears an outlier (perhaps because of highly reactive forms of iron (oxyhydr)oxides present in this surface layer, and the higher concentration of organic carbon fuelling sulfate reduction) and is not included in the main correlation shown. However, the data does indicate that in this sediment type an estimate of AVS should be possible from SPI images.

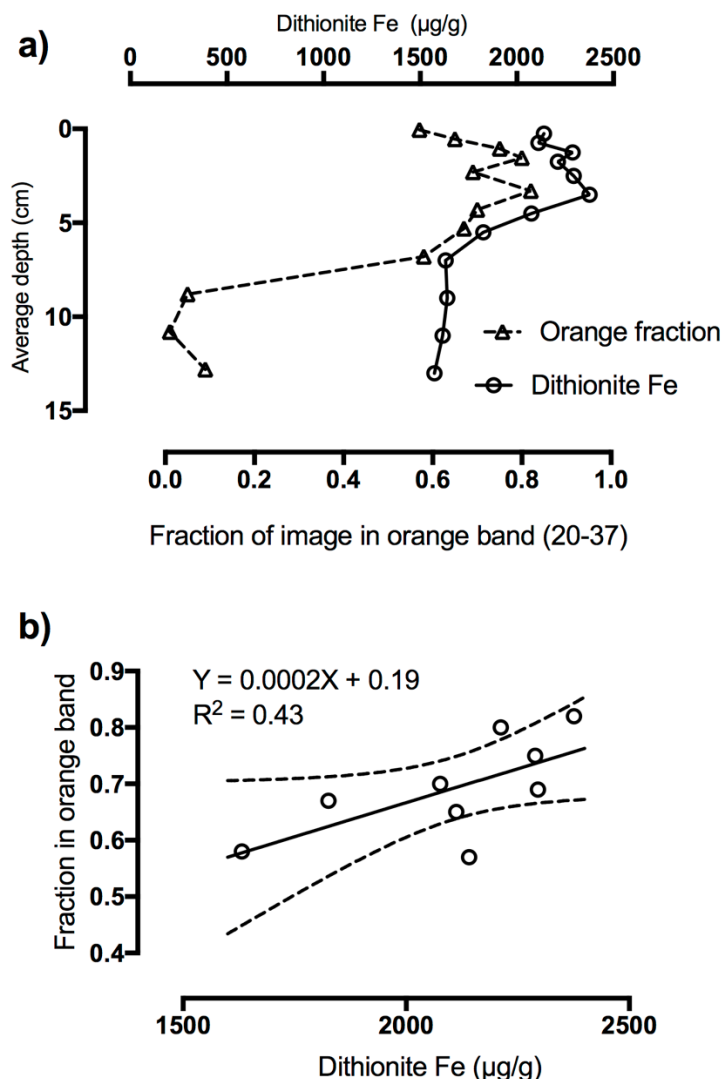
Figure 6. Acid volatile sulfur relative to core HSB brightness. Dotted lines are 95% confidence limits. Surface point omitted as appears an outlier.



For the iron (oxyhydr)oxides (dithionite-citrate leach) there is a modest correlation with the fraction of an image identified as orange in the zone above the aRPD (Figure 7). Below the aRPD there is no observable orange colour, presumably reflecting the formation of FeS at the

surface of oxides that obscures their colour. The relationship of leachable Fe with colour will depend on: 1) mineralogy of oxide phases with intermediate and mixed forms showing different orange colours, 2) the colour chosen for the image analysis (there was a shift to a more yellow colour with depth) and 3) any overlap of phases released by the leach technique. Given these limitations it is unsurprising that only a weak correlation was observed. However, the general trends in colour relative to the Fe phases measured in the upper part of the core, are clear (Figure 7).

Figure 7. a) Fraction of image in orange band and Fe dithionite leach data, with depth; b) correlation of orange fraction with dithionite leachable Fe in the zone above the aRPD.



The colour of complex mixtures of mineral phases is difficult to anticipate, but here where it is assumed that only two main coloured phases are present some success is achieved. Many sediment types are more complex, e.g. increased concentrations of sulfide phases caused by higher organic carbon content, and Mn rich systems where Mn oxides will impact colour. The illite here is relatively colourless but, reduced Fe incorporated into montmorillonite is reported to impart a green colour in reducing zones of open ocean sediments (Lyle, 1983), and if montmorillonite is present it may complicate interpretation.

A variety of factors in addition to those directly impacting colour may complicate interpretation in other shelf and coastal systems. Frequently, more complex structure than in the core discussed here may be seen, with, for example, localised zones of organic matter decomposition leading to intense carbon turnover that generates a halo effect of compressed redox zones. This zone is often visually manifested as a black colouration resulting from sulfate reduction and production of iron sulfide phases. Burrow structures that penetrate into reducing sediments and transport oxygen can also produce compressed redox features in their walls (Forster and Graf, 1992). Additionally, physical disturbances, including tidal mixing and trawling can perturb sediment structure and redox zones. However, the general concept of colour reflecting changes in the relative importance of the main coloured mineral phases within the sediment should still apply, even under these conditions where heterogeneity of the colour zones is increased.

4. Conclusions

The aRPD in the SPI image represents a significant visible change in the concentrations of the iron (oxyhydr)oxides and iron sulfide phases in the core, as has been shown by detailed analyses of the core solid phases and pore waters. Whilst both oxides and sulfur phases are present throughout the measured core depths the decrease in one and increase in the other leads to the net change in colour around the aRPD. It is important to note that in the shelf sediments studied here there is no obvious correlation between oxygen penetration and aRPD, and caution is needed in attempting to correlate colour changes with the depth to which oxygen penetrates (Gerwing et al., 2015).

The aRPD is a key component of the metrics that are increasingly used in, or under consideration for, management frameworks to assess seabed environmental health. These multi-metric indices include the OSI or Organism Sediment Index (Rhoads and Germano, 1986) and BHQ or Benthic Habitat Quality index (Nilsson and Rosenberg, 1997) and they or derivatives are finding use in, for example, the EU Water Framework Directive and Marine Strategy Framework Directive (Borja et al., 2008). The work reported here will help understand the aRPD so that its variability within these metrics or if used alone (Teal et al., 2010), and its relevance to biological communities, biogeochemical cycles and benthic ecosystem health will be better understood. Indeed, whilst the uncertainty around the nature of the aRPD remains, caution should be applied in using indices derived from it across regions where variability in factors impacting the aRPD are not fully understood. As Germano et al. recommended (2011) combining aRPD with other parameters in multivariate analyses might be a more appropriate approach. Further biogeochemical ground-truthing of the aRPD in other types of sedimentary systems with different sediment fabric, particle sizes and biological communities will inform and potentially extend its use further. It seems that the aRPD alone is something of a blunt tool for assessing ecosystem health and combination with other parameters is an important way ahead.

The correlation between AVS and SPI image colour may prove useful if estimates of sediment carrying capacity for toxic metals, e.g. Cu and Zn, and potentially other chalcophile elements, can be obtained from SPI spatial mapping within disposal sites. More work on the relative stability constants of these heavy metal sulfides and their formation in such sedimentary systems will be needed in this application. For more detailed geochemical interpretation of routine SPI images, development and application of new sensors and devices attached to SPI during deployment (e.g. oxygen penetration depth, pH, Fe/Mn, S), are needed

so that the range of parameters used in the assessment of seabed health can be extended.

5. Acknowledgements

This project was funded through Work Package 3 of the UK Shelf Sea Biogeochemistry Programme (NE/K001973/1 and NE/K001787/1), jointly funded by the Natural Environmental Research Council (NERC) and the Department for Environment, Food and Rural Affairs (Defra). The views expressed are those of the authors and do not necessarily represent those of NERC or Defra. W.B.H. was further supported by a NERC Fellowship (NE/K009532/1). The samples for this project were collected with the excellent support of captains, crew and NMF staff on the RRS *Discovery*. We are particularly grateful to fellow researchers within the SSB programme for providing assistance at sea. We express special thanks to Carolyn Harris for analysing nutrient samples during cruise DY034 and Malcolm Woodward for collating these data, Ross Williams for XRD work, David Chatelet (Biological imaging unit, University of Southampton) for help with ImageJ, Shir Akbari for POC/PIC analysis, and Matt Cooper for ICP-OES analyses. We are grateful for the useful comments provided by 2 anonymous reviewers that improved the manuscript.

6. References

- Albarede, F., 2003. Geochemistry- an introduction. Cambridge University Press.
- Bertics, V.J., Ziebis, W., 2009. Biodiversity of benthic microbial communities in bioturbated coastal sediments is controlled by geochemical microniches. *Isme Journal* 3, 1269-1285.
- Borja, A., Dauer, D.M., Diaz, R., Llanso, R.J., Muxika, I., Rodriguez, J.G., Schaffner, L., 2008. Assessing estuarine benthic quality conditions in Chesapeake Bay: A comparison of three indices. *Ecological Indicators* 8, 331-337.
- Bull, D.C., Williamson, R.B., 2001. Prediction of principal metal-binding solid phases in estuarine sediments from color image analysis. *Environ. Sci. Technol* 35, 1658–1662.
- Burdige, D.J., 2006. Geochemistry of marine sediments. Princeton University Press, Princeton, NJ.
- Canfield, D.E., Raiswell, R., Bottrell, S., 1992. The reactivity of sedimentary iron minerals toward sulfide. *American Journal of Science* 292, 659-683.
- Canfield, D.E., Raiswell, R., Westrich, J.T., Reaves, C.M., Berner, R.A., 1986. The use of chromium reduction in the analysis of reduced inorganic sulfur in sediments and shales. *Chemical Geology* 54, 149-155.

Devereux, R., Lehrter, J.C., Beddick, D.L., Yates, D.F., Jarvis, B.M., 2015. Manganese, iron, and sulfur cycling in Louisiana continental shelf sediments. *Continental Shelf Research* 99, 46-56.

Fenchel, T., 1969. The ecology of marine microbenthos. IV. Structure and function of the benthic ecosystem, its chemical and physical factors and microfauna communities with special reference to the ciliated Protozoa. *Ophelia* 6, 1-182.

Forster, S., Graf, G., 1992. Continuously measured changes in redox potential influenced by oxygen penetrating from burrows of callinassa-subterranea. *Hydrobiologia* 235, 527-532.

Germano, J.D., Rhoads, D.C., Valente, R.M., Carey, D.A., Solan, M., 2011. The use of sediment profile imaging (spi) for environmental impact assessments and monitoring studies: lessons learned from the past four decades, in: Gibson, R.N., Atkinson, R.J.A., Gordon, J.D.M. (Eds.), *Oceanography and Marine Biology: An Annual Review*, Vol 49, pp. 235-297.

Gerwing, T.G., Gerwing, A.M.A., Hamilton, D.J., Barbeau, M.A., 2015. Apparent redox potential discontinuity (aRPD) depth as a relative measure of sediment oxygen content and habitat quality. *International Journal of Sediment Research* 30, 74-80.

Grizzle, R.E., Penniman, C.A., 1991. Effects of organic enrichment on estuarine macrofaunal benthos - a comparison of sediment profile imaging and traditional methods. *Marine Ecology Progress Series* 74, 249-262.

Homoky, W.B., Weber, T., Berelson, W.M., Conway, T.M., Henderson, G.M., van Hulten, M., Jeandel, C., Severmann, S., Tagliabue, A., 2016. Quantifying trace element and isotope fluxes at the ocean-sediment boundary: a review. *Phil. Trans. R. Soc. A* 374:20160246.

Klar, J.K., Homoky, W.B., Statham, P.J., Birchill, A.J., Harris, E.L., Woodward, E.M.S., Silburn, B., Cooper, M.J., James, R.H., Connelly, D.P., Chever, F., Lichtschlag, A., Graves, C., 2017. Stability of dissolved and soluble Fe(II) in shelf sediment pore waters and release to an oxic water column. *Biogeochemistry*.

Lehto, N.J., Larsen, M., Zhang, H., Glud, R.N., Davison, W., 2017. A mesocosm study of oxygen and trace metal dynamics in sediment microniches of reactive organic material. *Scientific Reports* 7, 11369.

Lyle, M., 1983. The brown green color transition in marine-sediments - a marker of the Fe(III)-Fe(II) redox boundary. *Limnology and Oceanography* 28, 1026-1033.

Nieuwenhuize, J., Maas, Y.E.M., Middelburg, J.J., 1994. Rapid analysis of organic-carbon and nitrogen in particulate materials. *Marine Chemistry* 45, 217-224.

Nilsson, H.C., Rosenberg, R., 1997. Benthic habitat quality assessment of an oxygen stressed fjord by surface and sediment profile images. *Journal of Marine Systems* 11, 249-264.

Poulton, S.W., 2003. Sulfide oxidation and iron dissolution kinetics during the reaction of dissolved sulfide with ferrihydrite. *Chemical Geology* 202, 79-94.

Poulton, S.W., Canfield, D.E., 2005. Development of a sequential extraction procedure for iron: implications for iron partitioning in continentally derived particulates. *Chemical Geology* 214, 209-221.

- Poulton, S.W., Krom, M.D., Raiswell, R., 2004. A revised scheme for the reactivity of iron (oxyhydr)oxide minerals towards dissolved sulfide. *Geochimica Et Cosmochimica Acta* 68, 3703-3715.
- Raiswell, R., Canfield, D.E., Berner, R.A., 1994. A comparison of iron extraction methods for the determination of degree of pyritisation and the recognition of iron-limited pyrite formation. *Chemical Geology* 111, 101-110.
- Raiswell, R., Vu, H.P., Brinza, L., Benning, L.G., 2010. The determination of labile Fe in ferrihydrite by ascorbic acid extraction: Methodology, dissolution kinetics and loss of solubility with age and de-watering. *Chemical Geology* 278, 70-79.
- Rhoads, D.C., Cande, S., 1971. Sediment profile camera for in-situ study of organism-sediment relations. *Limnology and Oceanography* 16, 110-&.
- Rhoads, D.C., Germano, J.D., 1986. Interpreting long-term changes in benthic community structure: a new protocol. *Hydrobiologia* 142, 291-308.
- Rosenberg, R., Blomqvist, M., Nilsson, H.C., Cederwall, H., Dimming, A., 2004. Marine quality assessment by use of benthic species-abundance distributions: a proposed new protocol within the European Union Water Framework Directive. *Marine Pollution Bulletin* 49, 728-739.
- Seeberg-Elverfeldt, J., Schlüter, M., Feseker, T., Kölling, M., 2005. Rhizon sampling of porewaters near the sediment-water interface of aquatic systems. *Limnol Oceanogr.: Methods* 3, 361-371.
- Solan, M., Germano, J.D., Rhoads, D.C., Smith, C., Michaud, E., Parry, D., Wenzhofer, F., Kennedy, B., Henriques, C., Battle, E., Carey, D., Iocco, L., Valente, R., Watson, J., Rosenberg, R., 2003. Towards a greater understanding of pattern, scale and process in marine benthic systems: a picture is worth a thousand worms. *Journal of Experimental Marine Biology and Ecology* 285, 313-338.
- Solan, M., Wigham, B.D., Hudson, I.R., Kennedy, R., Coulon, C.H., Norling, K., Nilsson, H.C., Rosenberg, R., 2004. In situ quantification of bioturbation using time-lapse fluorescent sediment profile imaging (f-SPI), luminophore tracers and model simulation. *Marine Ecology Progress Series* 271, 1-12.
- Stookey, L.L., 1970. Ferrozine- a new spectrophotometric reagent for iron. *Analytical Chemistry* 42, 779-781.
- Teal, L.R., Parker, E.R., Solan, M., 2010. Sediment mixed layer as a proxy for benthic ecosystem process and function. *Marine Ecology Progress Series* 414, 27-40.
- Teal, L.R., Parker, E.R., Solan, M., 2013. Coupling bioturbation activity to metal (Fe and Mn) profiles in situ. *Biogeosciences* 10, 2365-2378.
- Teal, L.R., Parker, R., Fones, G., Solan, M., 2009. Simultaneous determination of in situ vertical transitions of color, pore-water metals, and visualization of infaunal activity in marine sediments. *Limnology and Oceanography* 54, 1801-1810.

Thamdrup, B., Fossing, H., Jorgensen, B.B., 1994. Manganese, iron, and sulfur cycling in a coastal marine sediment, Aarhus Bay, Denmark. *Geochimica Et Cosmochimica Acta* 58, 5115-5129.

Thompson, C.E.L., Silburn, B., Williams, M.E., Hull, T., Sivyer, D., Amoudry, L.O., Widdicombe, S., Ingels, J., Carnovale, G., McNeill, C.L., Hale, R., Marchais, C.L., Hicks, N., Smith, H.E.K., Klar, J.K., Hiddink, J.G., Kowalik, J., Kitidis, V., Reynolds, S., Woodward, E.M.S., Tait, K., Homoky, W.B., Kröger, S., Bolam, S., Godbold, J.A., Aldridge, J., Mayor, D.J., Benoist, N.M.A., Bett, B.J., Morris, K.J., Parker, E.R., Ruhl, H.A., Statham, P.J., Solan, M., 2017. An approach for the identification of exemplar sites for scaling up targeted field observations of benthic biogeochemistry in heterogeneous environments. *Biogeochemistry*.

Viollier, E., Inglett, P.W., Hunter, K., Roychoudhury, A.N., Van Capellen, P., 2000. The ferrozine method revisited: Fe(II)/Fe(III) determination in natural waters. *Applied Geochemistry* 15, 785-790.

Vismann, B., 1991. Sulfide tolerance - physiological-mechanisms and ecological implications. *Ophelia* 34, 1-27.

Woodward, E.M.S., Rees, A.P., 2001. Nutrient distributions in an anticyclonic eddy in the northeast Atlantic Ocean, with reference to nanomolar ammonium concentrations. *Deep-Sea Research Part II-Topical Studies in Oceanography* 48, 775-793.

Supplementary Material

1. TIFF high resolution version of core image
2. Data table (Excel spreadsheet)

Highlights

Sediment Profile Image directly linked to geochemical analyses

Colour of image related to iron phases in this core

Apparent Redox Potential Discontinuity (aRPD) not coincident with oxygen disappearance

Caution needed in use of aRPD in benthic sediment quality assessment indices